Nonlinear Conduction in Pure and Doped ZnO Varistors

A. Sedky, E. El-Suheel

Abstract—We report here structural, mechanical and I-V characteristics of $Zn_{1-x}M_xO$ ceramic samples with various x and M. It is found that the considered dopants does not influence the well-known peaks related to wurtzite structure of ZnO ceramics, while the shape and size of grains are clearly affected. Average crystalline diameters, deduced from XRD are between 42 nm and 54 nm, which are 70 times lower than those obtained from SEM micrographs. Interestingly, the potential barrier could be formed by adding Cu up to 0.20, and it is completely deformed by 0.025 Ni additions. The breakdown field could be enhanced up to 4138 V/cm by 0.025 Cu additions, followed by a decrease with further increase of Cu . On the other hand a gradual decrease in VHN is reported for both dopants and their values are higher in Ni samples as compared to Cu samples. The electrical conductivity is generally improved by Ni, while addition of Cu improved it only in the over doped region ($\geq$ 0.10). These results are discussed in terms of the difference of valency and ferromagnetic ordering for both dopants as compared to undoped sample.

Keywords—Semiconductors, Chemical Synthesis, Impurities and Electronic Transport

I. INTRODUCTION

ZINC oxide (ZnO) is well known for its non-stoichiometry due to the Zn atoms interstitial sites. It is commonly accepted that the ZnO exhibits an oxygen vacancies called intrinsic defects [1-4]. With these intrinsic defects, ZnO is an n-type semiconductor. These defects introduce donor states in the forbidden band slightly below the conduction band and reduce the energy gap (~ 3.2 eV) resulting in the conducting behavior of ZnO [5-8]. The interstitial neutral Zn atom is supposed to ionize two times respectively, and produce some of the free electrons [9,10]. Such free electrons move to the conducting band and enhance the ZnO conductivity, which can also be increased by any extrinsic defects which are obtained by dopants additions [11-14]. The donor density is about 10^{17} - 10^{19} / cm^3 and the grain resistivity is (0.1- 10 Ω.cm). While, the resistivity of grain boundaries is about 10^{10} - 10^{12} Ω.cm. Therefore, the current is mainly limited by the very high impedance of grain boundaries [1,3].

ZnO is an important in various fields of applications such as ceramics and varistors [15-17]. Polycrystalline ZnO with additives exhibits nonlinear current-voltage (I –V) characteristics because of electrostatic potential barriers formed at grain boundaries [18-22].

A.Sedky is with (a) Physics Department, Faculty of Science, King Faisal University, Al-Hassa 31982, P.O.B 400, Saudi Arabia. (b) Physics Deparment, Faculty of Science Assiut University, Egypt. E-mail: sedky1960@yahoo.com.
El-Suheel is with Physics Department, King Faisal University, Al-Hassa 31982, P.O.B 400, Saudi Arabia.

The existence of the nonlinearity region is the most significant property of the varistors due to its conducting phase in this region. The current increases much more quickly than the voltage and at high current density beyond 10^3 (A/cm²), the I-V curve exhibits an upturn region. The upturn region represents the voltage drop in the grains [1], and restricts ZnO varistors application. If donor doping reduces the grain resistivity, the voltage increase will be retarded and the upturn region will be delayed to higher current densities [23]. It is found that the nonlinear coefficient of ZnO mixed with several oxide additives may be achieved up to 80, and the breakdown field could be varied up to 5000 (V/cm) [2,25-28] . However, the nonlinear coefficient of ZnO remained inconvenient and still left the answer to the foresaid question open. The question arises whether nonlinear coefficient can be exceeding more than 80 or not.

In the use of electronic components such as varistors, the effects of dopants are very important because the electrical properties of ZnO are closely related to their composition and microstructure [29-35]. It has been reported that the doping has an effect, not only on the upturn region controlled by ZnO grains resistivity, but also on the low current region that determines the leakage current value. However, the low current region is mainly controlled by the grain boundaries, and the current has resistive I_R and capacitive I_c components such as $I_R << I_c$ [2].

Recently, we studied the current-voltage characteristic of ZnO samples with Fe and Mn as the magnetic additives [25,27]. It is found that addition of these additives improved the nonlinear properties of ZnO varistor and the electrical barriers could be formed, but the electrical conductivity is decreased. While the region of nonlinearity of ZnO can be extended to higher applied fields by Al and the conductivity of ZnO grains is improved [28]. On the other hand, mechanical properties of ceramic materials have important consideration in most of ceramic applications. It is well known that these materials have relatively weakly hardness, which limits the use of these materials in most of practical applications. One of the important methods to improve mechanical properties is the doping process. So, modification of mechanical properties of ZnO by additives will be tested for the first time to look more on the impact of these additives on the mechanical connection between grains. With this purpose in mind, a comparative study between the effects of magnetic (Ni) and nonmagnetic (Cu) dopants on structural, electrical and mechanical properties of ZnO is investigated. Interestingly, some important parameters such as valance state and magnetic moments of these dopants will be discussed , probably, for the first time in the present study. However, it is found that the potential barrier could be formed by adding Cu, and it is completely deformed by Ni addition. Furthermore, the

breakdown field could be enhanced up to 4138 V/cm , and also the electrical conductivity is improved.

II. EXPERIMENTAL

$Zn_{1-x}M_xO$ samples with various x and M ($0.00 \leq x \leq 0.20$ & M = Ni and Cu) are synthesized by using conventional solid-state reaction method [25-28]. The powders of ZnO, CuO and NiO (Aldrich 99.999 purity) are thoroughly mixed in required proportions and calcined at 1000^0 C in air for a period of 12 hours. The resulting powders are ground, mixed, pressed into pellets and sintered at temperatures of 1200 ^{o}C for 10 h in air. Finally, the samples are quenched down to room temperature. The bulk density of the samples is measured in terms of their weight and volume. The phase purity and surface morphology of the samples are examined by using X-ray diffractmeter (XRD) using Semen's D-500 with CuKα radiation of 1.541838 Å and scanning electron microscope JSM 5400 LV (SEM) equipped with energy dispersive X-ray microanalysis by resolution 157 eV (EDAX). I-V characteristics are obtained with an electrometer (model 6517, Keithley), 5 kV (300 mA) dc power supply and Omega digital multimeter. The samples are well polished and sandwiched between two cupper electrodes and the current is measured relative to the applied voltage. Finally, the microhardness of the samples is determined using an MH-6 digital microhardness tester 0.98 N.

III. RESULTS AND DISCUSSION

The bulk densities of the considered samples, listed in Table 1, are generally decreased by Ni and Cu addition as compared to undoped sample. The density of pure ZnO sample is consistent with the reported for ZnO (5.25 – 5.75). While, the decrease of density with doping addition may be related to some pores produced by dopants, in which the samples became more mass less. It is evident from the XRD patterns shown in Figure 1(a,b) that the structure of pure and doped samples is Wurtzite structure, and no additional peaks could be formed. The peaks (101) and (210) formed with more increase of Ni addition are also belong to Wurtzite structure of ZnO. The unidentified peak denoted by arrowhead could be seen only in the XRD pattern of 0.20 Cu samples. This confirm that both Ni and Cu dopants are substituted for Zn^{2+} in the unit cell, is the matching of ionic radii of Cu which are mixed from Cu^{2+} and Cu^{3+} (~ 0.72 Å) , and Ni^{2+} (0.69 Å) as compared to Zn^{2+} (0.74 Å). For a comparison between XRD and SEM analysis, the average crystalline diameter D_{hkl} is evaluated in terms of X-ray line broadening described by the following Scherrer's equation [36];

$$D_{hkl} = \frac{k\lambda}{\Delta\theta \cos\theta} \qquad (1)$$

Where λ is X-ray wavelength (λ = 1.5418 Ǎ), Δθ is half maximum line width, θ is Bragg angle and K is constant (K = 0.9 for this type of ceramics). The average values of D_{hkl} versus doping content are shown in Figure 1 (c). It is clear that the values of D_{hkl} are slightly decreased by the Ni doping addition up to 0.20, but it is increased by Cu except the
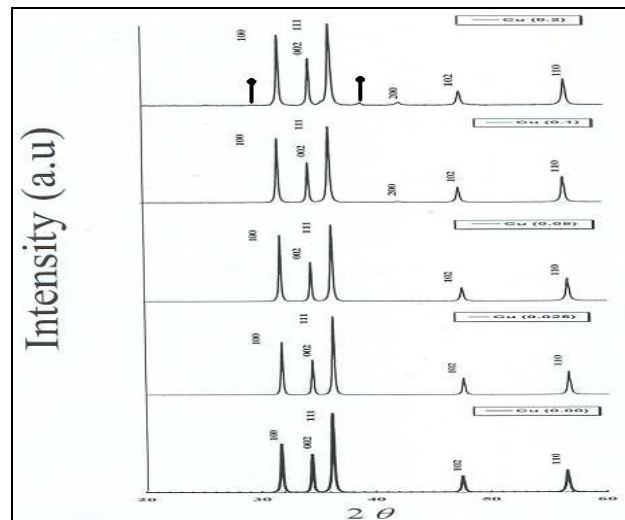
samples with Cu = 0.05 and Cu = 0.10 where D_{hkl} is decreased. However, the values of D_{hkl} are ranges between 42 nm to 54 nm for both dopants.

TABLE I
DENSITY, OF CU DOPED ZNO VARISTOR

Doping content	ρ (gm/cm^3)	Ni content	ρ (gm/cm^3)
0.00	5.37	0.00	5.37
0.025	3.82	0.025	3.61
0.05	3.88	0.05	2.88
0.10	3.53	0.10	2.68
0.20	3.59	0.20	3.70
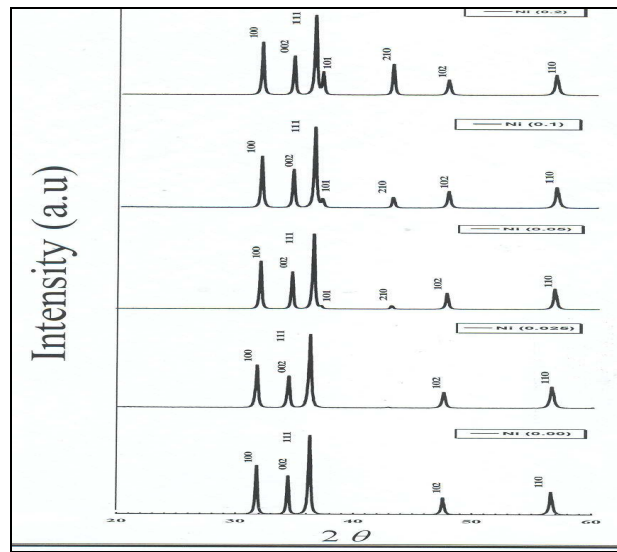
(a) XRD patterns of pure and Ni doped samples

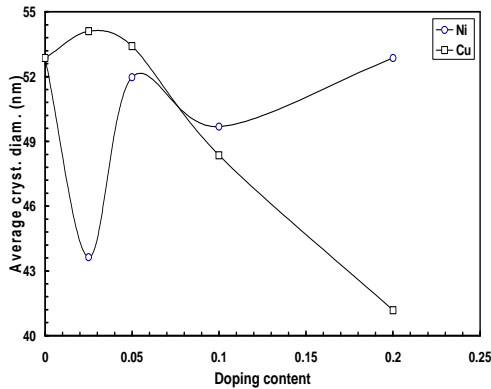(b) XRD patterns of pure and Cu doped samples

Fig. 1 (c) Average crystalline diameter versus doping content for Ni and Cu samples

Fig. 3 (a) Grain size versus doping content of $Zn_{1-x}M_x$ samples

Fig. 3 (b) Elements ratio for pure and Ni doped samples

Fig. 3 (c) Elements ratio for pure and Cu doped samples

The microstructure of pure and doped samples is shown in Figure 2. Nearly, no second phases are formed at grain boundaries, but the grains are randomly distributed and composed over the matrix structure. We are generally select 20 grains with different sizes to determine the average size for each sample. As shown in Figure 3 (a), both Ni and Cu increased the average grain size of undoped ZnO sample. The size of grains for Cu samples is nearly 1.5 times the same for Ni. The size of grains, deduced from surface SEM micrographs, are between 2.06 μm and 4.8 μm, which are 70 times higher than those obtained from XRD analysis. Although, some of scientists believe that equation (1) is not applicable to the grains larger than 100 nm, a previous studied of TEM analysis based on Ni doped ZnO varistors indicate that most of particles size is around 60 nm [36]. This is probably support average grain size deduced from XRD analysis rather than those obtained from SEM micrographs. The elements ratio, obtained from EDAX analysis, as a function of doping content is shown in Figure 3 (b,c). It is clear that the amount of both Cu and Ni are increase and Zn decreases.

The oxygen content is increased by doping addition, indicating a decrease of oxygen vacancies.
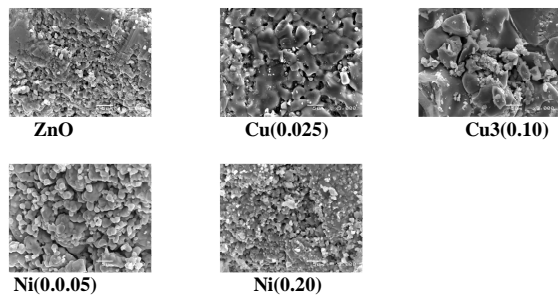

Fig. 2 The microstructure of pure and doped samples

The I-V curves of pure and doped samples are shown in Figure 4 (a,b). It is evident from the figures that there are three different regions observed in the I-V curves of pure and Cu doped sample. The first and third regions are nearly ohmic behavior, while the second region is clearly nonlinear behavior (upturn region). It is also noted that the second region (nonlinear region) is completely absent for Ni doped samples.
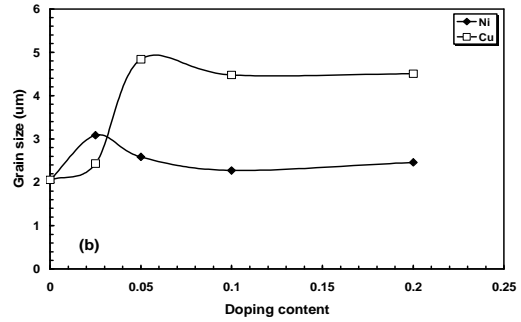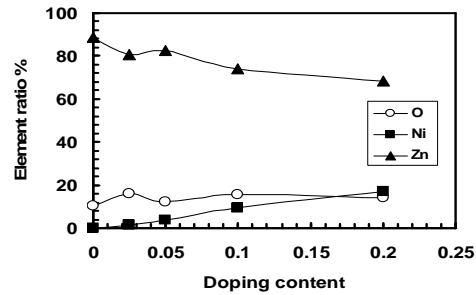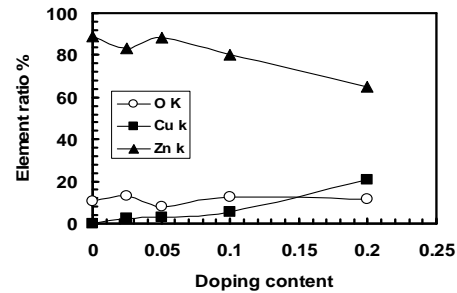
These results indicate that potential barrier could be formed by Cu addition, and it is deformed by Ni addition even at low doping content (0.025). The values of applied fields at the boundary of the nonlinear region for Cu doped samples are shifted to lowers values by Cu addition. While, the values of current density are generally increased by both dopants as compared to undoped sample. However, the important parameter, E_B breakdown field is usually taken as the field applied when the current flowing through the varistor is 1 mA/cm^2 [10,37]. The variation of E_B, obtained from dc electrical measurements, versus doping content is shown in Figure 4 (c). However, our facilities could not reach 1 mA/cm^2 for Cu = 0.025) sample, and the value of E_B is obtained from the extension of the third ohmic region which is plotted on a separate sheet. The breakdown field could be enhanced up to 4138 V/cm by 0.025 Cu doping followed by a decrease with further Cu addition up to 0.20. While, E_B can not exceeds 15 V/cm for Ni doped samples, which is lower than the value of E_B for pure sample . This of course is consistent with I-V

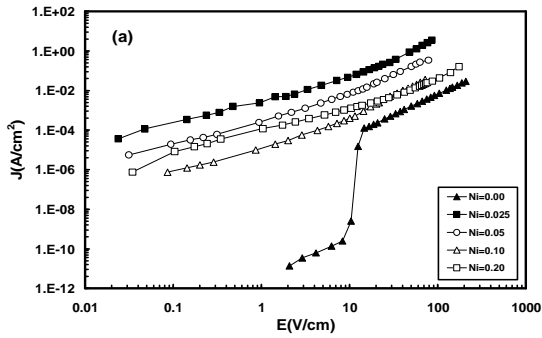measurements, where nonlinearity is completely absent for Ni doped samples.

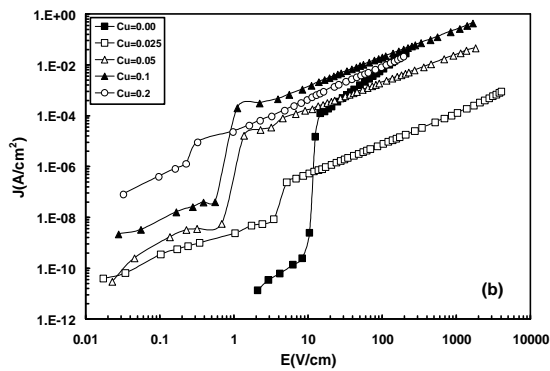Fig. 4 (a) I-V characteristics for pure and Ni doped samples

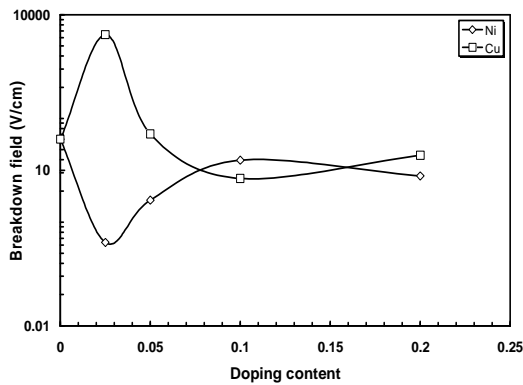Fig. 4 (b) I-Vcharacteristics for pure and Cu doped samples

Fig. 4 (c) Breakdown field versus doping content for $Zn_{1-x}M_x$ samples

The current - voltage relation of a varistor is given by the following equation [10,37];

$$J = (\frac{E}{C})^\alpha \qquad (2)$$

Where J is the current density, E is the applied electric field, C is a proportionality constant corresponding to the resistance of ohmic resistor (nonlinear resistance), α is the nonlinear coefficient (α = logV/logI). To obtain the value of α, the current - voltage curves are plotted on a log-log scale, from which the slope of the curve gives the value of α, as described in ref. [19,33]. The variation of α against doping content in the nonlinear region is shown in Figure 4 (d). It is apparent that values of α are decreased from 22.01 for pure sample to 8.25, 11.52, 12.28 and 5.43 with Cu addition, whereas it is remained close to 1 for all Ni doped samples. These values still very far than the achieved value 80 discussed above. From these results, it is determined that the addition of $Cu^{2+/3+}$ oxide to ZnO varistor composition decreased the non-ohmic features and shift the breakdown fields to higher values. While the nonlinear behavior disappeared by Ni^{2+} and the breakdown field is shifted to lower values.
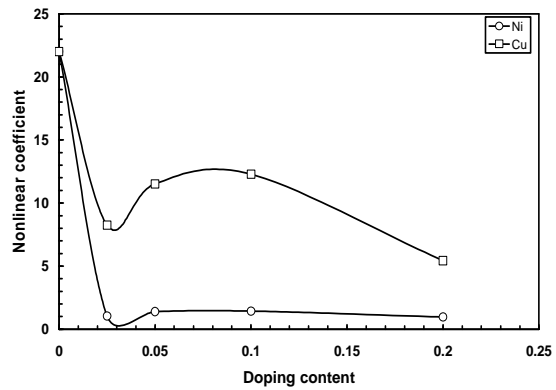

Fig. 4 (d) nonlinear coefficient versus doping content for $Zn_{1-x}M_x$ samples

This behavior is consistent with oxygen ration obtained from EDAX, where the oxygen vacancies controlling the formation barriers formed in ZnO varistors. On the other hand, the leakage current I_k corresponds to a field equal to half of breakdown field E_B [1,13,38]. Figure 4 (e) shows the variation of I_k against doping content for both dopaints. Although I_k is not systematic with the doping content, it is slightly higher for Ni samples than that of Cu samples, indicating higher barrier for Cu samples as compared to Ni samples.
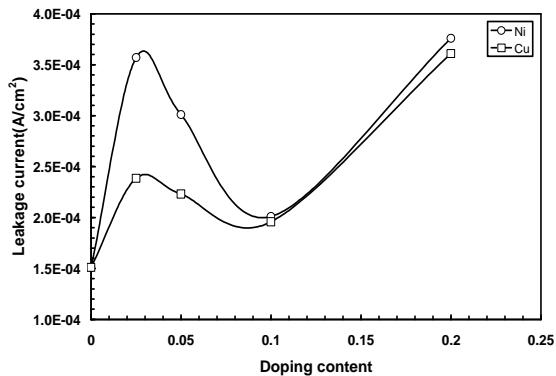

Fig. 4 (e) Leakage current versus doping content for $Zn_{1-x}M_x$ samples

Since Schottky type grain boundary barriers exist in the present samples, the current density in the ohmic region of

varistor is related to the applied electric field by the following formula [25,37];

$$J = AT^2 \exp\frac{(\beta E^{\frac{1}{2}} - \phi_B)}{K_B T} \qquad (3)$$

where A is the Richardson's constant $\{A = (4\rho e m K^2 / h^3)\}$, ρ is the varistor density, e is the electronic charge, m is the electronic mass, k is the Boltzmann constant, h is the Planks' constant, ϕ_B is the interface barrier height and β is a constant. By measuring the current density in the ohmic region and keeping the temperature constant, for two different roots of applied fields, the values of ϕ_B could be obtained. The variation of ϕ_B against doping content shown in Figure 4 (f) indicates that ϕ_B generally decreased by both dopants up to 0.20. This behavior is nearly consistent with the behavior of nonlinear coefficient, and vice versa with the behavior of breakdown field. These results supporting the deformation of electrical potential barriers by Ni in doped ZnO.
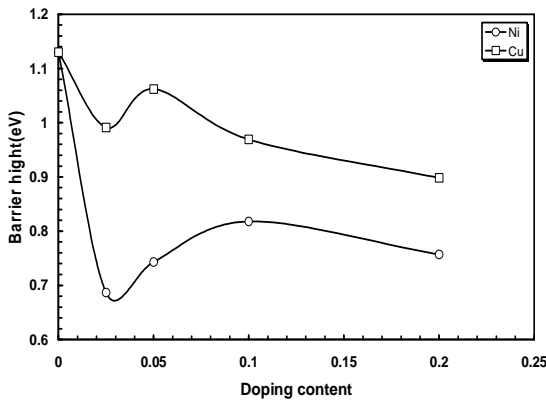

Fig. 4 (f) Barrier height versus doping content for $Zn_{1-x}M_x$ samples

In Zn substitutions with the considered doping, free electrons can released and raise the conductivity σ by increasing the electron density which are considered to be the majority carriers in the considered samples. In the present case, σ is calculated from the (J/E) in the first and third regions (ohmic regions). While, in the second region (nonlinear region), the current strongly increase due to the decrease of ϕ_B. Then, the conductivity in the nonlinear region is given by [39];

$$\sigma_2 = \sigma_1 \exp\{\frac{(\alpha - 1)(E_2 - E_1)}{E_2}\} \qquad (4)$$

Where σ_1 is the conductivity in the low field region (first reg.), E_1 and E_2 are the applied fields across the nonlinear region. Figure 5 (a-c) shows the dc electrical conductivity as a as a function of doping content across the three different regions. It is observed that the conductivity generally increased by the doping content as compared to ZnO sample , but the

rate of increase is higher in Ni samples than that of Cu samples. Anyhow, the conductivity curves could be divided into two regions as follows ; the first region at low doping content (0.00 $\leq$ M $\leq$ 0.05), in which the conductivity is increased by Ni and nearly unchanged by Cu ; whereas the second region where (0.10 $\leq$ M $\leq$ 0.2), in which the conductivity is nearly unchanged by doping content for both dopants.
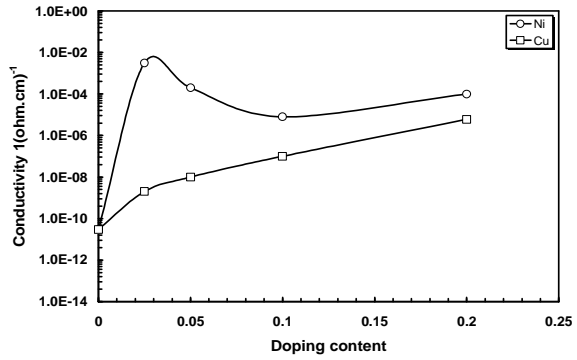

Fig. 5 (a): σ_1 versus doping content for $Zn_{1-x}M_x$ samples
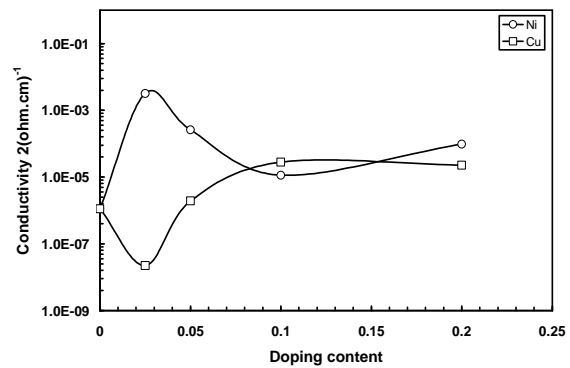

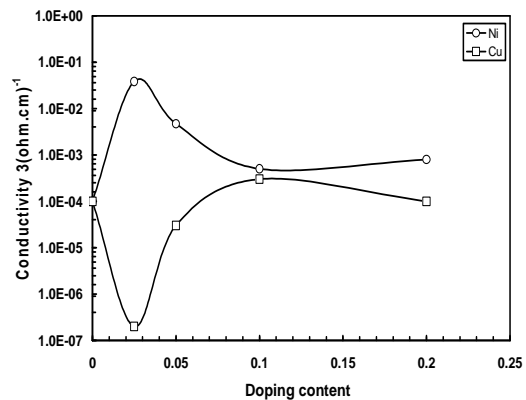Fig. 5 (b) σ_2 versus doping content for $Zn_{1-x}M_x$ samples

Fig. 5 (c) σ_3 versus doping content for $Zn_{1-x}M_x$ samples

The Vickers microhardness (VHN) is estimated according to the following relation;

$$VHN = 0.1891(\frac{P}{d^2}) \qquad\qquad (5)$$

where P is the applied load and d is the diagonal length of indenter impression. The value 0.1891 is a constant and represent a geometrical factor for the diamond pyramid. Anyhow, the above relation is taken from the menu of MH-6 tester. Figure 6 demonstrates the Vickers microhardness (VHN) plotted as a function of doping content at 0.98 N applied load. An approximately monotonically linear decrease in VHN with increasing doping content up to 0.20 is observed for both dopants. This means that the substitution up to 0.20 can substantially suppress microcrack of ZnO ceramics and consequently VHN is decreased. This is probably attributed to weakness of the coupling between the grains and elimination of pores, which may be occurs by the doping addition during heat treatments. Then, one can say that the mechanical resistance becomes lower and consequently the mechanical connection is depressed as result of pores discussed above. These results are consistent with the behavior of density against doping content. The question is why the values of VHN at low doping content (≤ 0.05) for Cu remain higher than the values of VHN for Ni, and vice versa for higher doping content. This is may be related to the difference in the values of density and grain size between dopants. To understand more about the VHN behavior against breakdown field, one can obtain a universal behavior between them.
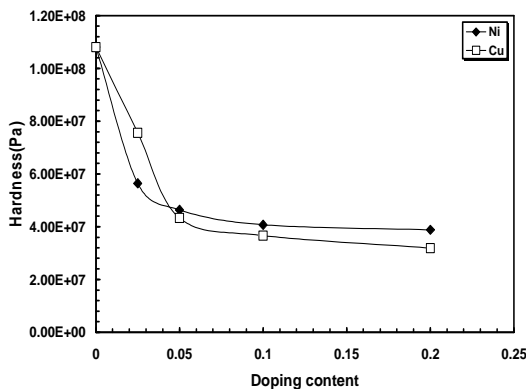

Fig. 6 Hardness versus doping content for $Zn_{1-x}M_x$ samples

However, it has been reported that the Cu-doped ZnO is more resistive, and the electrical conductivity is five orders of magnitude lower than that of ZnO [23]. But in the present case, electrical conductivity decreased significantly by the Cu-doping. However, it is proved that at high temperature over 1000 ^{0}C , the Cu valence could exist in ZnO as Cu^{+1}, which is supposed that Cu becomes more stable at high temperature. So, The Cu^{+1} ions are substituted for Zn^{2+} ions in the ZnO lattice and behave as an acceptor-type impurity [40-42]. Since the extrinsic donor is absent in the Cu-doped ZnO varistor, the Cu^{+1} ions has to be compensated by either intrinsic donor or hole doping to keep the electrical neutrality. Anyhow, the acceptors will be compensated by electrons in the grains because there are some intrinsic donors there. But the acceptors will be compensated by the holes in the grain boundary as a result of very low concentration of intrinsic donors there [43]. Moreover, the Cu dopants also had a great effect on the grain boundary as a result of interaction with ambient oxygen as the other 3-d transition metal impurity. Due to the above reasons, the Cu doped samples are more resistive than undoped sample. This explanation is in good agreement with our results only in the under doped region (Cu ≤ 0.025). But it is not correct in the over doped region , where the electrical conductivity is increased by Cu addition (Cu ≥ 0.05). Furthermore, the nonlinear coefficient decreased by 0.025 of Cu , followed by an increase with further Cu addition as well as in case of the behavior of breakdown field E_B against doping content . So, we believe that mixed of $Cu^{2+/3+}$ ions are substituted for Zn^{2+} in the ZnO lattice , behave as extrinsic donor dopants, and consequently the electrical conductivity will be increased. On the other hand, the Ni^{2+} dopants have a great effect on the grain boundary, but it makes the grains nearly non resistive as compared to undoped sample. In other words, Ni is considered as antidopant for the upturn region of ZnO, because it leads to deformation of the potential barrier in the grain boundary formed in the ZnO varistor. While the electrical conductivity increased by 0.025 Ni additions, followed by a decrease with further increase in Ni doping up to 0.20. But it is remains higher than undoped ZnO sample. Furthermore, the nonlinear region is completely absent by Ni addition even at 0.025 Ni content. Based on the above results, the question of barrier deformation by Ni addition is still open and the answer remains unclear. Anyhow, Ni is considered to be neutral dopants in ZnO since the Ni^{2+} ions are substituted for Zn^{2+} ions in the ZnO lattice, where 2^+ of Zn is replaced by 2+ of Ni. Therefore, both potential barrier and electrical conductivity should be unchanged, which could not obtained. However, it has been reported that diluted magnetic semiconductors are formed by partial substitution of n-type ZnO with small amount of magnetic transition metals such as Ni^{2+}. In $Zn_{0.95}Ni_{0.05}O$, ferromagnetic behavior at 300 K (0.29 μ_B) is observed [36,43]. Ferromagnetism is considered to originate from the exchange interaction between free delocalized carriers (holes or electrons from the valence band), and the localized d spins of Ni^{2+} ions [44]. We believe that order of ferromagnetism at 300 ^{o}K is the main reason for deformation of barriers of ZnO varistor by Ni addition. This may be occurs as a result of Ni magnetic moment which can be evaluated in the absence of extrinsic donors as discussed above. Based on the above, the difference in valence state and magnetic moment between Ni and Cu is responsible for the contrast in the behaviors of the two considered dopants, and also controlling the nonlinearity of ZnO varistors.

IV. CONCLUSION

Structural, mechanical and electrical properties of ZnO ceramic varistor doped by Ni and Cu transition metals are investigated. We have shown that both dopants does not influence the well-known peaks related to wurtzite structure of ZnO ceramics; whereas the shape and size of grains are clearly affected. The potential barrier could be formed by adding Cu, and it is completely deformed by Ni addition. The breakdown

field could be enhanced up to 4138 V/cm by 0.025 Cu doping. A gradual decrease in VHN is reported for both dopants, but its values for Ni doped samples are higher than Cu. The electrical conductivity is generally improved by Ni, while addition of Cu improved it only in the over doped region ($\geq$ 0.10). We believe that the order of ferromagnetism at 300 ^{o}K produced by Ni is the main reason for deformation of potential barriers of ZnO varistor. Furthermore, the valence state and magnetic moment are found to be responsible for controlling the nonlinearity of ZnO varistors.

REFERENCES

[1] T.K. Gupta, J. Am. Ceram. Soc. 73, 1817 (1990).
[2] A.B. Glot, J. Mater. Sci.: Mater electron 17, 755 (2006).
[3] L.M. Levinson and H. R. Phillip, Am. Cream. Soc. Bull. 65 (4) 639 (1986).
[4] G.D. Mahan, L.M. Levinson, H.R. Philipp, J. Appl. Phys. 50, 2799 (1979).
[5] B.Z.Azmi, Zahid Rizwan, M. Hashim, A.H. Shaari, W.M.M. Yunus and E. Saion, Am. J. Appl. Sci. (Special Issue) , 22 (2005).
[6] V. Srikant and D.R. Clarke, J. Appl. Phys. 83, 10, 5447 (1998).
[7] Q. Shen, T. Toyoda, Jpn. J. Appl. Phys. 39, 3146 (2000).
[8] S. Abdalla; K. Easawi; T. A. El-Brolossy, G. M. Yossef, S. Negm and H. Talaat, Rev. Sci. Instrum., 74 No (1), 848 (2003).
[9] T.K. Gupta, J. Mater. Res. 7 (12), 3280 (1992).
[10] Mourad Houabes, Slavko Bernik and Chabance Talhi and Ai Bui, Ceramic international 29, (6), 783 (2005).
[11] A.M.R Senos, M.R. Santos, A.P. Moreira and J.M. Vieira, In surface and Interfaces of Ceramic Materials, ed. L. C. Dufour, C. Monty and G. Petot-Ervas, NATO ASI Series, Kluwer Academic, London, 553 (1988).
[12] A.M.R Senos and J.M. Vieira, In Proceedings of the international Conference Third Euro-Ceramics, Vol 1, ed. P. Duran and J. F. Fernandez, Faenza Edit rice Iberica S. L. Faenza, 821 (1993).
[13] J.D. Levine, CRC Crit. Revs. Solid States Sci. 5, 597 (1975).
[14] J. Bernasconi, S. Strassler, B. Knecht, H.P. Klein and A. Menth, Solid State Communs. 21, 867 (1977).
[15] N.W.Emanetoglu, C.Gorla, Y.Liu, S.Liang and Y.Lu, Mater.Sci. Semicond. Process. 2, 247 (1999).
[16] R.Paneva and D.Gotchev, Sens. Actuators A: Phys. 72, 79 (1999).
[17] Lian Gao, Qiang Li , Weiling Luan, Hirokazu Kawaoka, Tohru Sekino and Koichi Niihara , J.Am. Ceram. Soc. 85, 4, 1016 (2002).
[18] D.R. Clarke, J.Am. Ceram.Soc. 82, 3, 485 (1999).
[19] M. Matsouka, Jpn.J. Appl. Phys. 10, 6, 736 (1971).
[20] K. Mukae, K. Tsuda and I. Nagasawa, Jpn.J. Appl. Phys. 16, 8, 1361 (1977).
[21] G.E. Pike and C.H. Seager, J.Appl. Phys., 50, 5, 3414 (1979).
[22] Fumiyasu Obe, Yukio Sato, Takahisa Yamamoto, Yuichi Ikuhara and Taketo Sakuma, J.Am. Ceram. Soc. 86, 9 , 1 (2003).
[23] Zhen Zhou, K. Kato, T. Komaki, M. Yoshino, H.Yukawa, M.Morinaga and K.Morita , J. Eur. Ceram. Soc. 24 , 139 (2004).
[24] A.Sedky, M.Abu-Abdeen and Abdul-Aziz A. Almulhem, Physica B 388, 266 (2007).
[25] A. Sedky , Ayman Al- Sawalha and A.M. Yassin, Physica , Egyption J . Solids 31, 2, 205 (2008).
[26] A.Sedky, T.A. El-Brolossy and S.B. Mohamed , J. Phys. Chem. Solids 73, 505 (2012).
[27] A.Sedky and E. El-Suheel , Physics Research International, 2010, 1 (2010).
[28] A. Sedky , Ayman Al- Sawalha and A.M. Yassin, Physica B 404 , 3519 (2009).
[29] J. Han, P.Q. Mantas and A.M.R. Senos, J. Eur. Ceram. Soc. 21, 1883 (2001).
[30] J. Han, A.M.R. Senos and P.Q. Mantas, J. Eur. Ceram. Soc. 22 , 1653 (2002).
[31] J. Han, A.M.R. Senos and P.Q. Mantas, J. Eur. Ceram. Soc. 19 , 1003 (1999).
[32] J. Han, A.M.R. Senos and P.Q. Mantas, Mater. Chem. Phys. 75 , 117 (2002).
[33] J. Han, P.Q. Mantas and A.M.R. Senos, J. Eur. Ceram. Soc. 22 , 49 (2002).
[34] D.C.Look, J.W. Hemsky and J.R. Sizelove, Phys. Rev. Lett. 82, 2552 (1999).
[35] W.G. Carlson and T.K.Gupta, J.Appl. Phys. 53, 5746 (1982).
[36] Guangqing Pei, Changtai Xia, Shixun Cao, Jungang Zhang, Feng Wu and Jun Xu, JMMM 302, 2, 340 (2006).
[37] V.V. Deshpande, M.M. Patil and V. Ravi, Ceramic international 32, 85 (2006).
[38] T. Takemura, M. Kobayashi, Y. Takada and K. Sato, J.Am. Ceram. Soc. 70, (4), 237(1987).
[39] A.Sedky, Under Press, Superlattice and Microstructures (2011).
[40] P. Fons, K. Nakahara, A. Yamada, K. Iwata, K. Matsubara, H. Takasu and S. Niki, Phys. Stat. Sol. 229,2 , 849 (2002).
[41] T.R. Kutty and N. Raghu, Appl. Phys. Lett. 54, 18, 1796 (1989).
[42] S.T. Jun and G.M. Choi, J. Am. Ceram. Soc. 81, 3, 695 (1998).
[43] T. Dietl, Semicond. Sci. Technol. 17, 377 (2002).
[44] K.R. Kittilstved, N.S. Norberg, D.R. Gamelin, Phys. Rev. Lett. 94, 147209 (2005).